Smart Structures and Systems, *Vol. 15, No. 3 (2015) 577-592*
DOI: http://dx.doi.org/10.12989/sss.2015.15.3.577

Can we substitute the intuition of an experienced bridge inspector by monitoring?

Helmut Wenzel[*1], Hiroshi Tanaka[2a], Michaela Höllrigl-Binder[1] and Helga Allmer[1]

[1]*VCE Vienna Consulting Engineers ZT GmbH, Hadikgasse 60, 1140 Vienna, Austria*
[2]*University of Ottawa, 161, Louis Pasteur St., A115, Ottawa, Ontario, K1N 6N5, Canada*

(Received November 27, 2014, Revised January 18, 2015, Accepted January 20, 2015)

Abstract. Damage quantification is a major goal of the SHM community. Methodologies to introduce a quantity for actual condition of a structure into the assessment process are desired. The idea that the condition of a structure is represented in the character of its dynamic response is fully accepted by the SHM community. The VCLIFE methodology quantifies condition analyzing input from monitoring.

Keywords: SHM; Monitoring

1. Introduction

Experienced bridge inspectors are able to express a first condition assessment shortly after having visited a bridge which normally proves to be rather reliable. What we call intuition might be experience-driven human sensing of bridge performance. The human body is sensitive to vibration and classifies the excitation it is exposed to. On the other hand, we as humans, change our behavior when we feel pain indicating damage. The same happens to bridge structures. In case of damage the load paths modify. This is reflected in the response of the structures to ambient and forced vibrations. Model based observer monitoring concepts use this approach and actually measure what human intuition tells us. The approach and technology described below provide background information as well as examples of successful application.

Dedication to Yozo Fujino

I met Yozo Fujino more than 20 years ago at an IABSE event and was impressed by his knowledge of and approach to bridge assessment. He is one of those experienced engineers who are called when complicated and high profile cases arise. Since that first encounter we have discussed the subject of bridge assessment many times and both worked in damage detection. I am delighted to dedicate some of our later results, developed in the IRIS project, to Yozo Fujino and his achievements.

∗Corresponding author, Professor, E-mail: wenzel@vce.at
[a] Ph.D.

http://www.techno-press.org/?journal=sss&subpage=8 ISSN: 1738-1584 (Print), 1738-1991 (Online)

2. Structural non-linearity and energy transfer

The concept described in this chapter has been developed within the large European research project IRIS and comprises only a portion of the methodology. The complete work is documented in (Wenze 2013) and available for download under www.vce.at/iris .

The findings described herein have been discussed within our research group including myself (concept and approach), Hiroshi Tanaka (fluid dynamics), Helga Allmer (physics and mechanics) and Michaela Höllrigl-Binder (mathematics). We were looking into the subject from the point of view of energy transfer in a changing system over time. Our approach was tested in many cases by destructive testing and published it in journals and conferences. We are glad to report that the idea has been taken up by many research groups and is frequently quoted in respective publications.

Cascading energy transfer in a dynamical system could be caused by the development of nonlinear characteristics of the structural response caused by various reasons.

Suppose a nonlinear mechanism develops in both the damping and stiffness of a structure, whose dynamic behavior is modeled by a Single Degree of Freedom (SDOF), as a result of progressive structural damage. Fig. 1 illustrates the progress of such damage.

It can be typically represented by the equation of motion by modifying both the damping and stiffness terms as follows

$$m\ddot{z} + c[1 + \varepsilon_2(z)]\dot{z} + k[1 - \varepsilon_1(z)]z = 0 \tag{1}$$

where ε_1 and ε_2 are the linear or nonlinear correction terms introduced corresponding to the development of structural damage and $z(t)$ represents the dynamic response of the structure in general. Note that it is unlikely to have any change in the inertia term. Eq. (1) can be rewritten as

$$m\ddot{z} + c\dot{z} + kz = k\varepsilon_1(z)z - c\varepsilon_2(z)\dot{z} = F(z,\dot{z}) \tag{2}$$

where $F(z,\dot{z})$ is generally a nonlinear function of z and/or $\dot{z}$, such as

$$F(z,\dot{z}) = C_1 z^2 + C_2 \dot{z}^3 \tag{3}$$

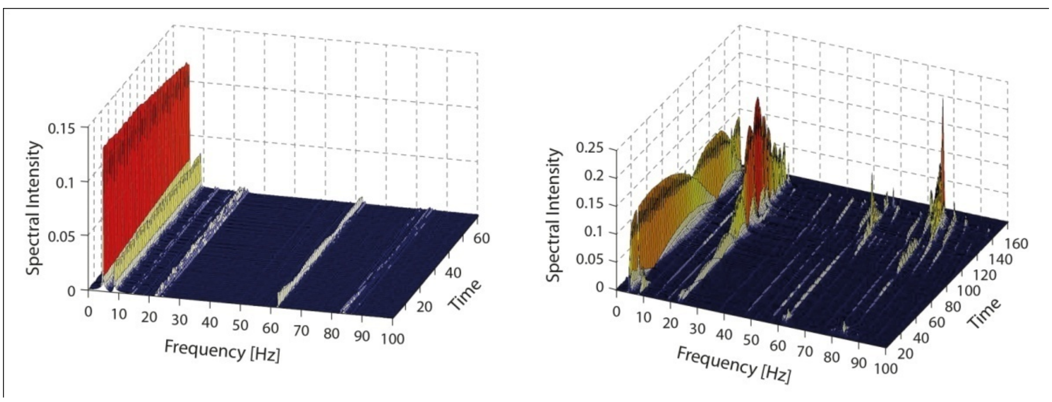

Fig. 1 Spectral development over time for a sound structure (left) and during a damage test at MPA Stuttgart (right)

Eq. (3) implies that if z is modeled as a vibration with frequency ω, then $F(z,\dot{z})$ is generally a function of fluctuations with the frequencies expressed by the multiples of ω. For example, substitution of $z = A\sin\omega t$ in Eq. (3) obtains Eq. (4).

$$F(z,\dot{z}) = \frac{C_1A^2}{2}\left(1-\cos 2\omega t\right) + \frac{C_2A^3\omega^3}{4}\left(3\cos\omega t + \cos 3\omega t\right) \tag{4}$$

This in turn will result in a dynamic response represented by functions of twice, thrice higher frequencies than the original ones for this case. The same process will be repeated as time allows and, as a result, a part of the system's dynamic energy will be gradually distributed to an increasingly higher frequency range.

Where would this process end? For the case of damage-caused nonlinearity, the high frequency energy components dissipate as heat or noise and, if not, the destruction or rupture of the structure would play a role. Even if it does not reach the destruction point, the mechanism of structural response will change significantly when damage progresses that far.

3. The energy cascade in turbulence

Energy cascading, such as the one described in the preceding section, can be associated with various types of nonlinear physical phenomena. It is typically observed in dynamics of turbulent fluid flow. The process of energy cascading is one of the most central issues in the case of fully developed turbulence.

The English physicist L.F. Richardson (1881-1953) conceived of turbulence as an assembly of eddies of different sizes, where eddies could be hypothetically visualized as individual vortices of some measurable diameter. He had the idea that large eddies are prone to break into smaller eddies, which break up into even smaller eddies and so on as spelled out by the following famous parody:

> "Big whirls have little whirls
> That feed on their velocity,
> And little whirls have lesser whirls
> And so on to viscosity." - by L.F. Richardson (1922)-

In each break-up process, the larger eddy transfers its dynamic energy to the smaller ones without dissipating it, meaning that the energy transfer process in turbulence is inviscid. In such a process, the role of viscous forces is negligible in comparison to the inertia forces. However, energy has to be eventually dissipated somewhere, at much smaller wave lengths, or higher frequencies. This is a viscous process. Fluid viscosity has an important role only at those small scales.

This process can be modeled mathematically as follows: the Navier-Stokes equation is a non-linear equation because of an inherent non-linearity of fluid inertia as shown in Eq. (5)

$$\rho\left(\frac{\partial u_i}{\partial t} + u_j\frac{\partial u_i}{\partial x_j}\right) + \frac{\partial p}{\partial x_j} = \frac{\partial}{\partial x_j}\left(\mu\frac{\partial u_i}{\partial x_j}\right) \tag{5}$$

Out of the three terms involved in the equation, the pressure gradient can be ignored in the present discussion. In the energy dissipation process described herein, the inertia term becomes less important in comparison to the viscous force in higher frequency range, and hence the whole equation becomes almost linear for this case, whereas at much larger length scales, or in the lower frequency range, the inertia term becomes predominant and hence the equation becomes highly non-linear. This is where cascading takes place. Note therefore that the non-linear characteristics of the equation, in particular of the inertia force for this case, are deeply associated with the energy cascading phenomena explained by Richardson.

4. Nonlinear damping

Relationship of energy cascading as a result of advancing nonlinearity in a dynamical system is therefore evident in two different phenomena. A very interesting aspect of this conclusion is that the detection of energy cascading could be potentially utilized as a tool for the structural health monitoring. The traditional idea of knowledge-based structural health monitoring focused on identifying the reduction of stiffness, which proved to be far less sensitive than desired for practical purposes. In contrast, by finding the transfer of dynamic energy to higher frequencies through spectral analysis of ambient vibrations, it may be possible to detect damage development in a structure at its earlier stages. Any extent of structural damage can of course change the local structural damping or energy dissipation and stiffness. As a consequence, the global dynamic properties of the structure, i.e., the eigenfrequencies, mode shapes and modal damping would be all somewhat influenced.

It must be kept in mind that structural nonlinearity is attributed, not only to developing damage. Field experience indicates that the magnitude of modal damping is often amplitude-dependent. Damping increases with amplitude due to energy consumption at friction bearings, bending action of piers, behavior of the bridge outfitting as well as the structure-vehicle interaction (Wenzel 2009).

Admittedly the present method would also detect the developing structural nonlinearity due to large motion. However, if there is a development of structural damage as its consequence, the nonlinear characteristics would be retained by the structure after the large amplitude motion disappeared and should be thus detected.

5. Data analysis

For identifying the energy cascading phenomena, the following data analysis can be applied.

5.1 Data preparation

Acceleration signals $a_i(t)$ are measured for a period of $t_i \le t \le t_i + T$, where $i = 1,2,...,n$, with the sampling frequency and measuring period of typically $f_S = 500\,\mathrm{Hz}$ and $T = 5\,\mathrm{min}$, respectively. n is the number of files.

5.2 Analysis

Calculation of the acceleration spectra $G_i(f)$ by a conventional FFT routine for the frequency range of $0 \le f \le f_M$ is required first. $f_M = f_S/2$ is the folding frequency. The *normalized spectral density functions* are then calculated as shown in Eq. (6).

$$F_i(f) = \frac{G_i(f)}{\sigma_i^2} \qquad \text{where } \sigma_i^2 = \sum_f G_i(f)\Delta f \tag{6}$$

Normalization of spectral density is justified since our interest is only in the change of energy distribution pattern and not in the actual magnitude of the spectral density, which depends on the total dynamic energy supplied by excitation and is always expected to change during the ambient vibration survey. It is also useful to calculate the fraction of dynamic energy corresponding to less than any particular frequency level f as shown in Eq. (7).

$$E_i(f) = \sum_{k=0}^{f} F_i(k)\Delta k \tag{7}$$

where $E_i(f)$ is the *spectral distribution function* which is expected to more clearly reveal the fraction of energy transferred to different frequency ranges, resulting in the change of its pattern.

5.3 Presentation

Visual presentation of $F_i(f)$ and $E_i(f)$ with respect to time (i) and frequency (f) would indicate the transfer of energy to higher frequencies by the change in spectral pattern, where $1 \le i \le n$ and $0 \le f \le 250$ Hz.

5.4 Reading of spectral patterns

When the distribution function $E_i(f)$ is examined, it should be noted that the energy cascading caused by structural nonlinearity discussed herein is only a partial transfer of energy through the free vibration process of the structure. As stated in Section 2 not all dynamic energy is transferable to high frequency range. Some of the energy should remain with the lower vibration modes.

Another important point is that during the vibration survey various dynamic excitations or disturbances from the external environment may act on the structure. As a result, new dynamic energy will be supplied to the system augmenting the energy fraction at corresponding frequencies. The characteristics of these excitations are often hard to identify. However, when there are any predominant excitation frequencies, there may be distinct spectral peaks observed at those particular frequencies. If the excitation resembles broad-band noise, a part of this energy will be absorbed at eigenfrequencies and corresponding spectral peaks will show up as additional spikes in the figures.

The change of pattern in $E_i(f)$ is, therefore, not expected to be monotonous. Hence, what needs to be observed is a general tendency of the energy shift, which, it is hoped, will be indicated by a gradual change of the colored pattern.

The shift of pattern can be quantified by locating the centroid of the area under the spectral distribution $E_i(f)$ as shown in Eq. (8).

$$\bar{r} = \sum_f fE_i(f)\Delta f \Big/ \sum_f E_i(f)\Delta f \tag{8}$$

The shift of the centroid is unlikely to be monotonous. What should be observed is the general tendency of its change.

6. Example: Overpass S101, Reibersdorf (2008)

The following example is based on the measurement of dynamic bridge response carried out in December 2008 for the highway overpass S101 in Reibersdorf, Upper Austria. The structure was progressively damaged prior to its demolition, in order to observe the effects on the dynamic characteristics [1]. Sampling frequency of the acceleration record was 500 Hz.

Figs. 2 and 3 depict the progressive change of the normalized acceleration spectrum $F_i(f)$ and the distributed spectrum $E_i(f)$ for the frequency range of $0 \le f \le 25$ Hz from the measured results. There were a number of physical operations applied to the bridge during three days of measurement. Some of them are specified next to the figures. Some of these operations can be clearly identified from the patterns of the functions $F_i(f)$ and $E_i(f)$. When the concrete pier or slab is being cut, presumably the severing operation produced large extent of high frequency noise and, consequently, a large fraction of the total dynamic energy appears in a much higher frequency range as a substantial spike in $E_i(f)$. In the afternoon of the third day, for example, there was "a vibrating roller working next to the bridge, causing clearly noticeable vibrations on the bridge", according to the measurement report. This noise may be also contributing to the above mentioned spikes.

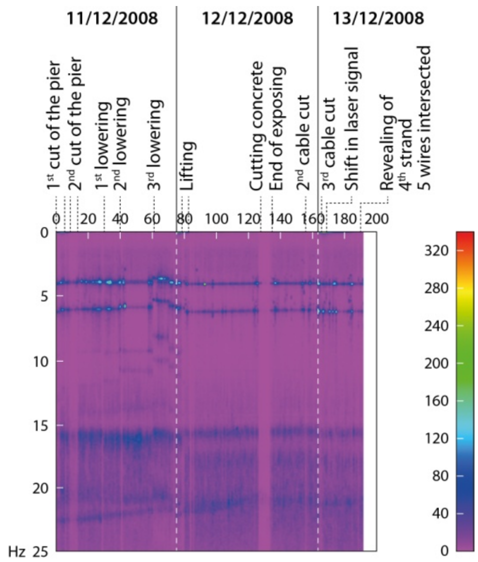

Fig. 2 Normalized acceleration spectra $F_i(f)$

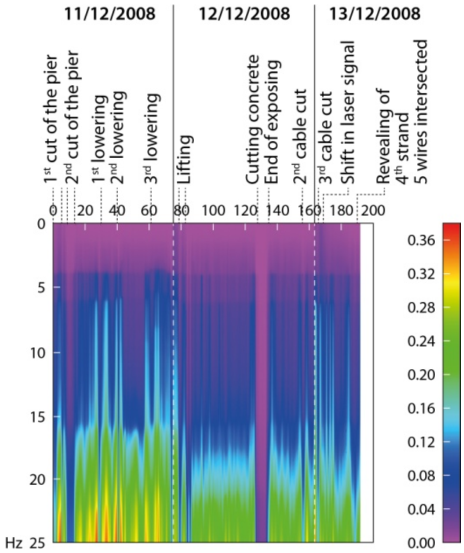

Fig. 3 Spectral distribution functions $E_i(f)$

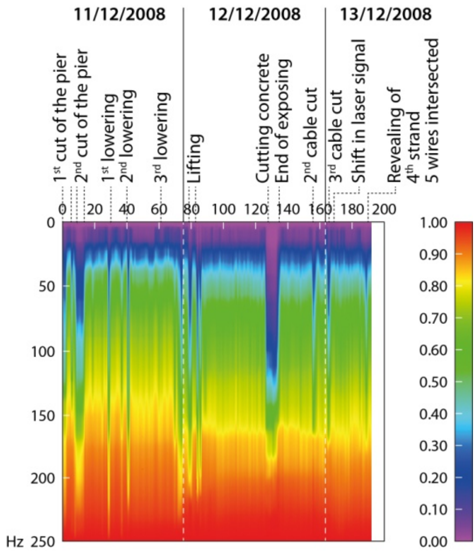

Fig. 4 Spectral distribution functions $E_i(f)$

It is clear by observing the $E_i(f)$ pattern that, with the progressive damage artificially induced in the bridge, an increasing fraction of dynamic energy was redistributed to the higher frequency range, as indicated by the shift of dark blue and yellow band towards right, meaning the higher percentage fraction is in the high frequency side of the figure. Fig. 4 is the same $E_i(f)$ function shown for much wider frequency range up to 250 Hz. It is clear that an almost stepwise energy shift took place after the lifting of the damaged pier in the beginning of the second day.

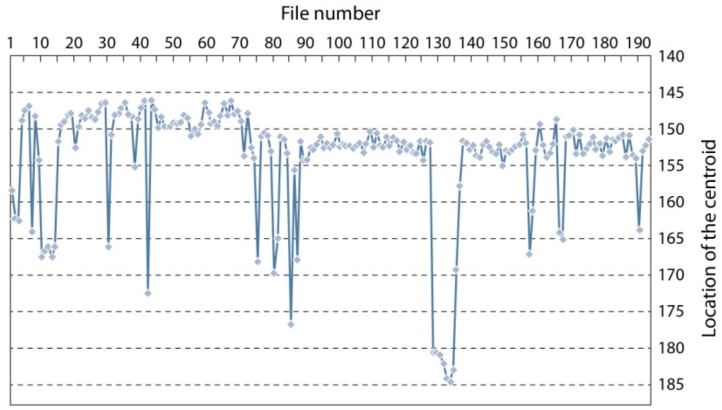

Fig. 5 Normalized acceleration spectra $F_i(f)$

The same tendency is demonstrated even more clearly by calculating the shift of the centroid $\bar{r}$ of the area under $E_i(f)$ as shown in Fig. 5. By disregarding the spikes due to various kinds of noise, the general trend is clearly one of shifting towards a higher frequency range with time.

6.1 Further discussion on the test results

Fig. 6 shows some changes in the 1st and 2nd eigenfrequencies during these three days, most likely caused by the change in bridge's physical conditions. What is shown as "Amplitude" indicates the ordinate of the normalized spectra at this particular frequency, namely the modal intensity of the dynamic energy. Artificial damage of the bridge pier was applied on the North-West column of the bridge and the measurements B and C were taken at the mid-span of the bridge on West and East side, respectively.

It is evident that there were two steps of frequency reduction, though the second one is less clear, corresponding to the cutting of the pier on the first day. This was the first damage induced in the bridge. Immediately following the second cut, the structure recovered its first mode frequency but not the second mode. Note that the column was still maintained at its original elevation by jacking. The measurement report (Wenzel *et al.* 2009) states that "no restoring forces observed" for the same period. A most conspicuous loss of stiffness, both in the first and second modes, took place during the lowering of the pier. During that period it was observed that a part of the dynamic energy started being clearly transferred to the higher frequency range. This corresponds to the reported development of cracks in the structure due to its settlement. The recovery of both frequencies on the second day corresponds to re-lifting of the column and the insertion of steel plates under it. Substantial transfer of energy is observed compared to the previous day. The plot of the modal energy (shown as "Amplitude"), also shows that only a small fraction of energy remains associated with the first and the second modes through this period. The gradual reduction of both frequencies through the day may have been caused by the change of ambient temperature or a gradual settling of the structure. The further cascading process seems to be associated with the cutting of concrete slab and steel tendons. It is interesting to observe that no change of the first and second eigenfrequencies was observed during this operation.

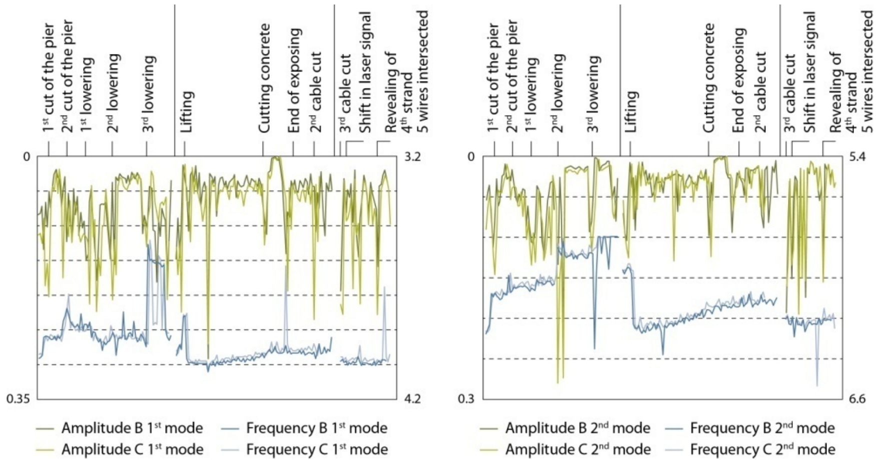

Fig. 6 Change of the 1st (left) and 2nd (right) frequency

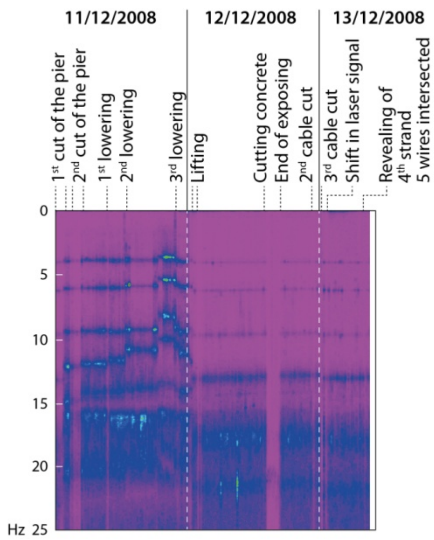

Fig. 7 Normalized acceleration spectra Fi(f) on the pier

The third tendon was severed on the third day and apparent re-settling of the structure was stated in the measurement report. Further transfer of dynamic energy is obvious in Fig. 3, though again this operation had no visible effects on lower eigenfrequencies.

Another set of spectral presentations, Figs. 8-10, results from the acceleration record obtained directly above the damaged pier. The general tendency of the reduction of eigenfrequencies and energy transfer towards high frequency range, is the same as seen in the preceding results, but it can be observed even more clearly with this set of data. What is clearly different from the other sets of data are the conspicuous spectral peaks in the frequency range of $8 \leq f \leq 13$ Hz. Explanation of these peaks is not immediately provided.

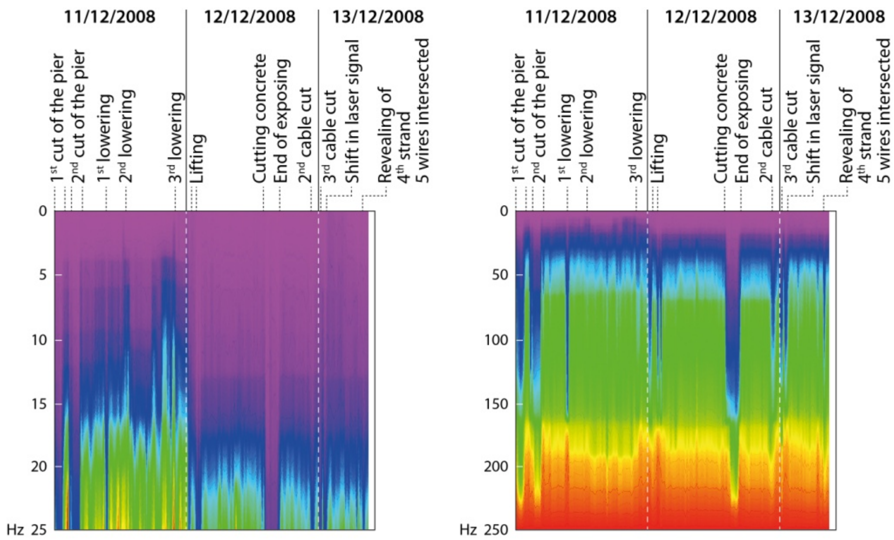

Fig. 8 Spectral distribution functions $E_i(f)$ on the pier

7. Other sample cases

The proposed spectral analysis method for damage identification seems to be successful at least in the case of the S101 overpass. Admittedly, however, the case was rather ideal. The scheduled damage was successively applied to the structure and the measurement was carried out in a controlled environment, without disturbances, such as on-going traffic. Nevertheless, after the encouragement of this initial success, the method has been further tried out on other bridges. A brief summary of sample cases follows.

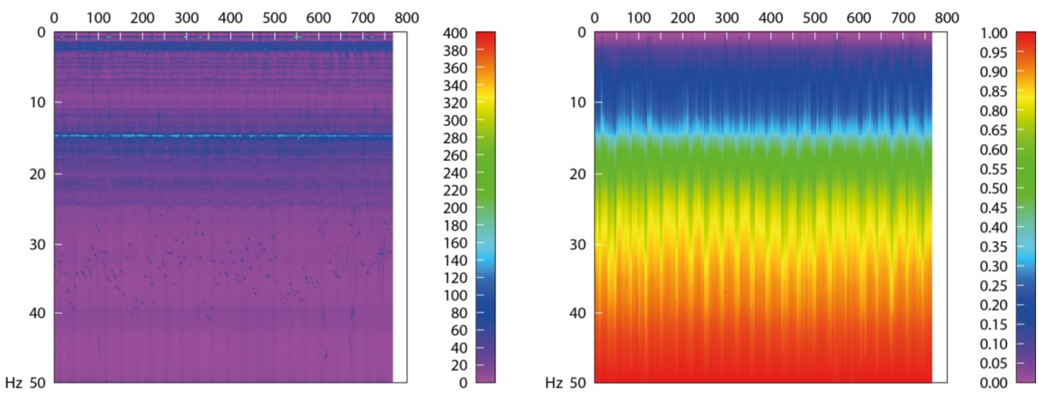

Fig. 9 Europabrücke: based on midday records

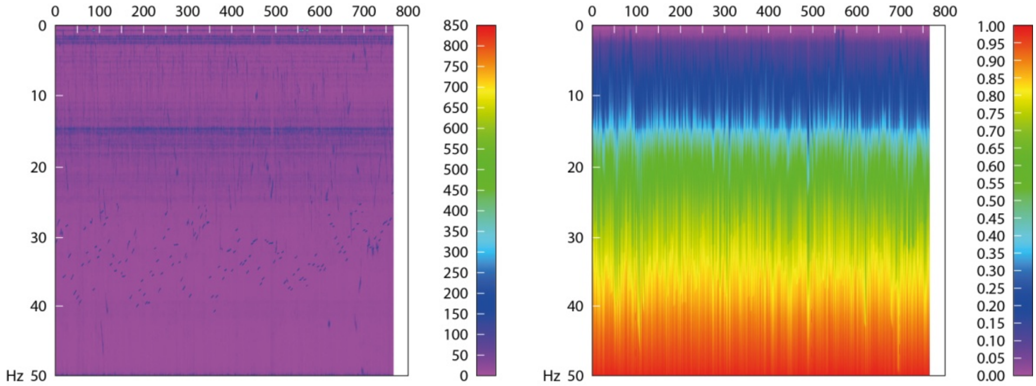

Fig. 10 Europabrücke: based on midnight records

7.1 Europabrücke (2005)

The Europabrücke, opened in 1963, is one of the main alpine north-south routes for urban and freight traffic. It currently carries over 30000 motor vehicles per day. The superstructure is a steel box girder of variable height along the span with an orthotropic deck. The bridge is 657 m long and consists of six spans of different length, carrying six lanes, three in each direction, with a total width of 25 m. In order to assess the prevailing vibration intensities with regard to possible fatigue damage, a permanent measuring system has been installed since 2003. Extensive records of vibration measurement exist. Figs. 9 and 10 represent the analyzed results of the records from May to October 2005, at middays and midnights, respectively. They show a basically healthy, stable condition of the structure, with no indication of serious structural non-linearity.

The statistical evaluation of the data reveals a significant change of the pattern for 80% of the energy after the 4th week of observation, but the whole plot shows a fluctuation that might be due to different traffic. Fig. 11 shows the boxplots of midday and midnight results.

It must be kept in mind, however, that the existence of structural non-linearity, in stiffness and/or damping, is not necessarily 100% equivalent to a state of structural damage. There may be a case where micro-cracks are developing, for example, but the overall structural behavior does not show any sign of nonlinearity.

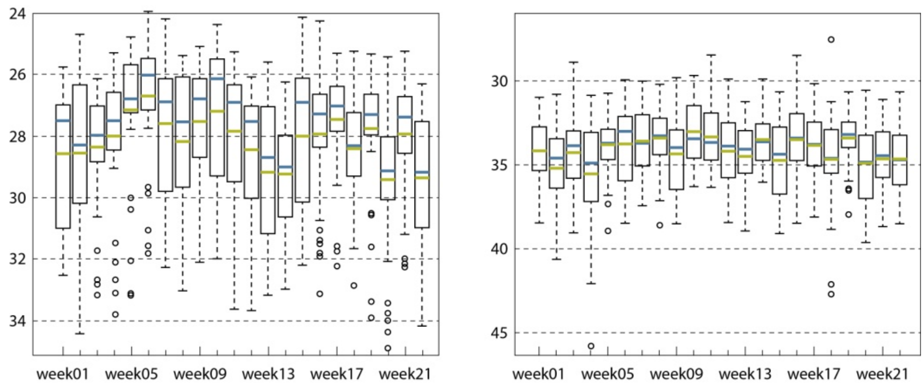

Fig. 11 Europabrücke: midday (left) and midnight (right) – boxplot of 80% of energy

7.2 Melk B3A (2000–2009)

This is an example of a structure deteriorating over a period of nine years. Disregarding some irregularities, the gradual change of the spectral pattern (Fig. 12) clearly indicates that more and more dynamic energy is transferred towards higher frequency ranges.

In looking at the change in spectral patterns, it is important to compare the cases of the same structure under similar physical conditions. For example, all measurements of this particular bridge were carried out under its service conditions, namely under traffic loads. Since traffic loads tend to enhance the bridge vibration in a certain limited range of frequency, the resulted spectral pattern is different from that obtained under more random ambient excitations such as micro-tremors or wind. Under such conditions, the spectra tend to shift towards a lower frequency range compared to conditions without traffic. In order to avoid this effect, an effort was made to extract some data obtained when the bridge was freely vibrating without traffic loads. The resulting spectral pattern without traffic excitation is shown in Fig. 13.

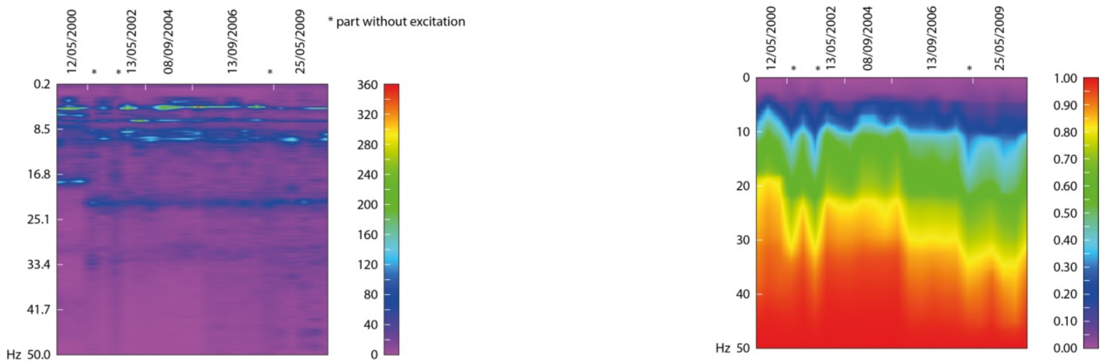

Fig. 12 Melk B3A

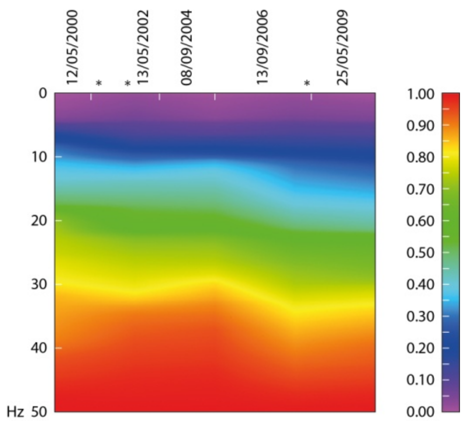

Fig. 13 Melk B3A: without traffic

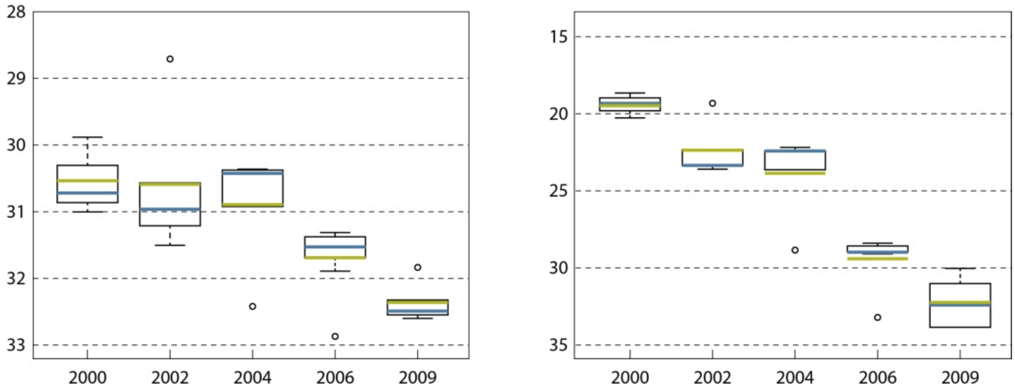

Fig. 14 Melk B3A: boxplot of the centroid (left) and boxplot of 80% of the energy (right)

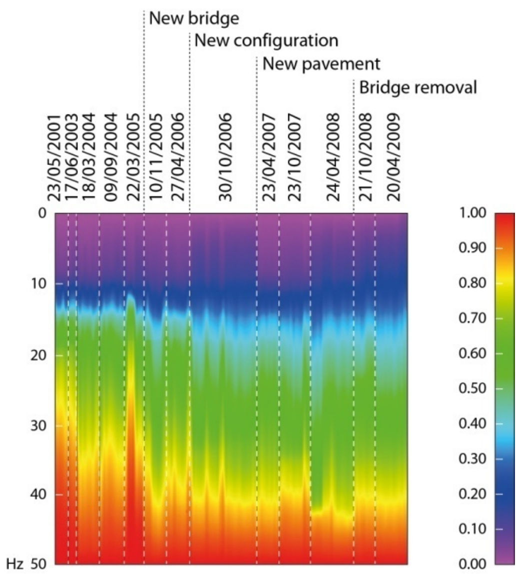

Fig. 15 Flughafen

Concerning the statistical evaluation of this bridge, it depends on which value is used. For this bridge the results of the location of the centroid of the energy distribution and the value of 80% of energy are presented to show that there can be a difference: significant changes for this structure can be observed with the analysis of variance (ANOVA) for the location of the centroid from the 5th observation period (that is the year 2006) and for the value for 80% of energy from the 4th observation period (that is the year 2004). Fig. 14 shows the boxplots of these results.

7.3 Flughafen Vorfahrt (2004–2009)

The access bridge in front of the terminal 2 of the Vienna International Airport was opened in 1956 and widened to 10.5 m in 1968. Measurements of the dynamic characteristics took place after a concern was expressed regarding its load carrying capacity. Available data are from eleven different groups of files accumulated over a period of five years, March 2004 through April 2009, while the construction work was progressing. There were a number of changes in structural configuration, therefore, over this period (Furtner 2009). Regardless of the history of various events occurring at the structure, there is clearly a general trend of dynamic energy shift towards higher frequency ranges throughout the period (Fig. 15).

The first 33 of the existing data files were sampled at a frequency of 100 Hz and the last 98 files at 500 Hz. When the sampling frequency was 100 Hz, any spectral information in high frequencies beyond 50 Hz would have been lost. An important question is whether any meaningful engineering judgment could be made based only on the information of less than the cut-off frequency. The effects of sampling rates on the depicted spectral patterns were examined, because of this reason, based on the data of this bridge only from the last 98 files, by comparing the following two cases:

// for $0 < f \leq 50$ Hz by re-sampling the data at 100 Hz, namely every fifth points and

// for $0 < f \leq 250$ Hz based on the data available at 500 Hz sampling.

Figs. 16 and 17, (A) and (B) compare the normalized spectra $F_i(f)$ and the cumulative distribution $E_i(f)$ of both cases. Transfer of energy to a higher frequency range that took place between various events is clearly better recognized by the results of (B). The high spectral peaks started appearing in the higher frequency range after milling of the ramp started in April 2007, indicating a significant change of spectral pattern. In terms of the cumulative spectral energy $E_i(f)$, it is more clearly recognized by case (B), rather than (A), since presumably more and more energy is transferred to the frequency range beyond 50 Hz. Note, however, that high frequency noise is also effectively cut off for the case of (A) due to low sampling frequency and it sometimes makes it easier to look at the color pattern since the spikes caused by operational noise are reduced.

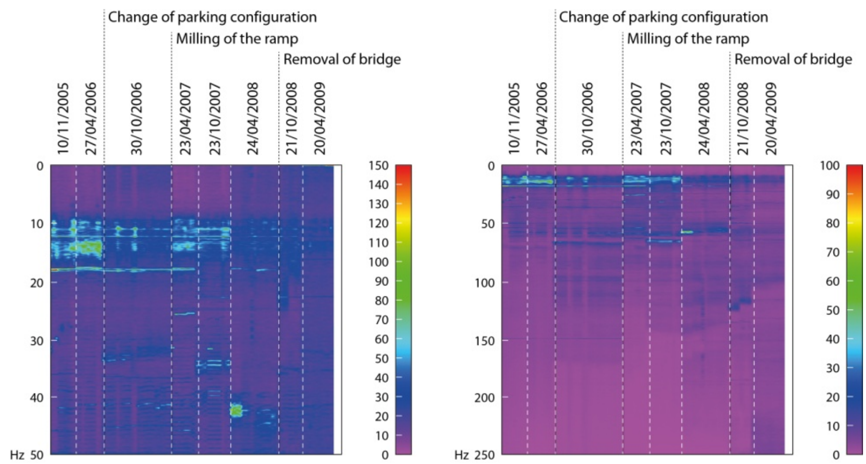

Fig. 16 Flughafen: $F_i(f)$ the last 98 files (A) and (B)

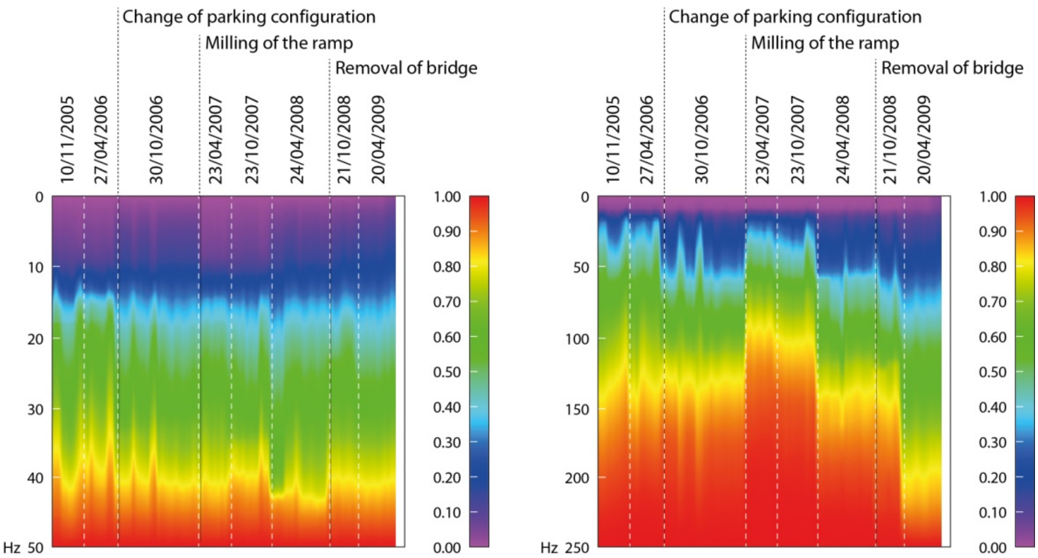

Fig. 17 Flughafen: $E_i(f)$ the last 98 files (A) and (B)

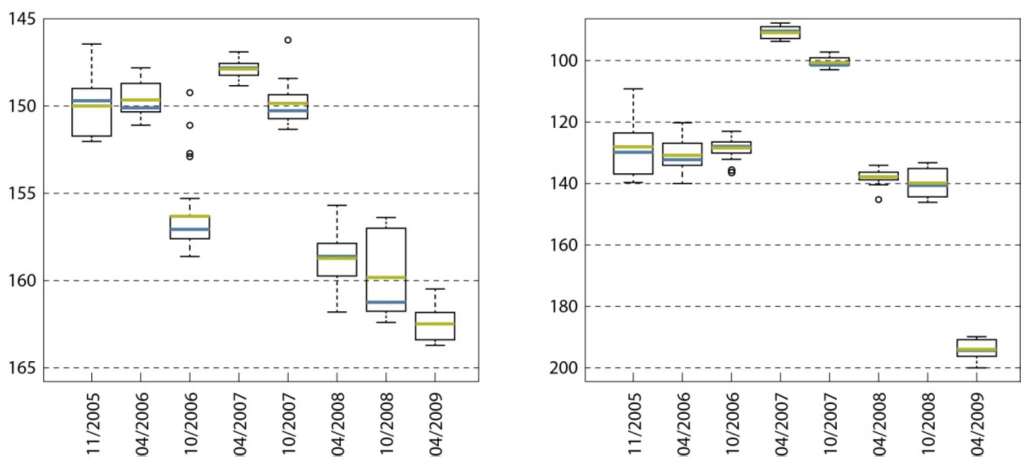

Fig. 18 Flughafen: boxplot of the centroid (left) boxplot of 80 % of the energy (right)

The statistical analysis obtains significant changes for this structure with the analysis of variance (ANOVA) for the location of the centroid from the 3rd observation period (that is the year 2006) and for the value for 80% of energy from the 4th observation period (that is the year 2004). Fig. 18 shows the boxplots of these results.

8. Conclusions

The proposed spectral method (VCLIFE) was applied to on-site measurement data at several different bridges. The results presented herein indicate a possibility of effectively detecting the development of structural damage by looking at the change of the spectral pattern due to the shift of dynamic energy towards a higher frequency range. It should be noted that the results are more informative when the sampling frequency is high enough, generally speaking.

The energy shift seems to be quite characteristic to the structures with developing damages. It is believed that a combination of the ambient vibration survey and the proposed spectral analysis can be an effective and simple structural health monitoring tool. To this end, it would be ideal if a criterion for the extent of structural damage corresponding to any indicator of the energy shift can be established. Locating the centroid of the area under $E_i(f)$ curves is one possibility but its validity would require further investigation.

A sampling frequency of 500 Hz is recommended for future measurements. For identifying the high frequency shift of dynamic energy, it is desirable to minimize the effects of extraneous disturbances, particularly those of traffic load. Ideally, if the spectrum of excitation force can be identified even approximately, its contribution towards the output spectra can be estimated, however, this is not the case most of the time. Minimization of noise effects could be achieved by taking a long enough record so that undesirable noise, including the traffic load, can be regarded more or less an evenly distributed excitation. Taking several consecutive files, each 330 seconds long, would suffice. Ideally, the free vibration record of the structure should be observed over a certain period of time. Importantly any measurements involving multiple locations on a structure should be made with respect to a fixed reference point throughout the project.

References

Furtner, P. (2009), Flughafen Wien Schwechat Vorfahrt Ost Terminal 2 – Objekt 102, Dynamische Charakteristik der Bauwerke, Periodische Nachmessung und Interpretation der Ergebnisse. Report 09/1042, April 2009.

Wenzel, H. (2009), *Health Monitoring of Bridges*, J. Wiley and Sons Ltd., Chichester – England, ISBN 9780470031735, 2009.

Wenzel, H. et al. (2013), *Industrial Safety and Life Cycle Engineering*, VCE Vienna Consulting Engineers ZT GmbH, Vienna, Austria, ISBN 9783200031791, 2013.

Wenzel, H. and Pichler D. (2005), *Ambient Vibration Monitoring*, J. Wiley and Sons Ltd., Chichester – England, ISBN 0470024305, 2005.

Wenzel, H., Veit-Egerer, R., Widmann, M. and Jaornik, P. (2009), WP3 Demonstration Report. Deliverable D11.1, October 2009.